A Technique to Measure Submillimeter Tokamak Synchrotron Radiation Spectra

R. A. BLANKEN, P. BROSSIER, AND D. S. KOMM

Abstract—**A wire-mesh Fabry–Pérot interferometer with millisecond response time has been constructed. The application of this instrument to study the millimeter and submillimeter synchrotron radiation emitted by magnetically confined Tokamak plasmas is discussed.**

I. INTRODUCTION

THE STUDY of the synchrotron radiation emitted from present-day Tokamak experiments is important for several reasons. First, synchrotron radiation losses could play an important role in the energy balance of such plasmas. Second, the spectrum can yield diagnostic information about the electron-temperature profile and the runaway population. The predicted emission spectrum is discussed in Section II.

Since present day experiments occur on a time scale of tens of milliseconds the spectral information should be obtained in times shorter than 10 ms. For this purpose we have developed a fast-scanning Fabry–Pérot interferometer which is described in Section III.

The application of this instrument to the analysis of synchrotron radiation spectra for typical Tokamak experiments is discussed in Section IV.

II. SYNCHROTRON RADIATION FROM EXPERIMENTAL TOKAMAK PLASMAS

The power spectrum of the radiation emitted by a charged particle spiraling in a magnetic field B was first derived nonrelativistically by Schott in 1912 [1]. The relativistic treatment was given by Schwinger [2]. Tokamaks lie in the so-called nonrelativistic regime $n\beta \ll 1$, where n is the harmonic number of radiation, and $\beta \equiv v/c$, where v and c are the particle velocity and the speed of the light, respectively. Within this limit the total power radiated by one electron of charge e and mass m_e in a given harmonic n, assuming $\beta_{\|} \equiv v_{\|}/c = 0$, is given by [3]

$$n_\omega = \frac{e^2\omega_c^2}{2\pi\epsilon_0 c}\frac{(n+1)\,(n^{2n+1})}{(2n+1)\,!}\beta^{2n}\ \mathrm{W} \tag{1}$$

where $\omega_c = \omega_c(x) = eB(x)/m_e$ is the electron cyclotron frequency. The volumetric emission coefficient j_ω is obtained by integrating over the electron distribution function. For a Maxwellian velocity distribution

$$j_\omega = \int f(\boldsymbol{v})\eta_\omega\, d^3v = \frac{\omega_p^2\omega_c^2}{2\pi c^3}\,2kT_e\,\frac{(n+1)\,(n^{2n+1})}{(2n+1)\,!}\cdot\left(\frac{2kT_e}{m_e c^2}\right)^{n-1}\ \mathrm{W\cdot m^{-3}} \tag{2}$$

where n_e and $\omega_p = (n_e e^2/\epsilon_0 m_e)^{1/2}$ are the electron plasma density and plasma frequency, respectively. The assumption $\beta_{\|} = 0$, while it produces small errors in the total radiated power, has the major effect of producing a spectrum consisting of a series of δ functions at $n\omega_c$, since the Doppler broadening of the spectrum is completely neglected. Experimentally, the only effect of the Doppler broadening will be to impose a limitation on the spatial resolution obtainable (see Section IV).

To calculate the power loss from the plasma the reabsorption of the emitted radiation must be considered. One must therefore solve a ray equation for the intensity I

$$dI/dx = j_\omega - \alpha_\omega I \tag{3}$$

where α_ω is the spatial-absorption coefficient. The solution is given by

$$I = (j_\omega/\alpha_\omega)\left[1 - \exp\left(-\int_{\text{ray path}}\alpha_\omega\, dl\right)\right]. \tag{4}$$

In thermal equilibrium, of course,

$$j_\omega/\alpha_\omega = B_0(\omega) = \omega^2 kT/8\pi^3c^2\ \mathrm{W\ sr^{-1}\ (rad/s)^{-1}\ m^{-2}} \tag{5}$$

where $B_0(\omega)$ is the blackbody intensity in the Rayleigh–Jeans limit ($\hbar\omega \ll kT$). Equation (4) shows that for a Maxwellian electron distribution function, the emitted radiation cannot exceed the blackbody level.

Numerous calculations of the energy losses from thermonuclear plasmas have been made using (4), assuming the magnetic field is constant [4]. Rosenbluth [5] first considered an inhomogeneous magnetic field and found increased radiation losses. Recently, the inhomogeneous-field losses have also been studied in more detail by Engelmann and Curatolo [6]. While these calculations are informative, they consider only a single pass of the ray through the plasma. In the experiments, the emitted rays are reflected from the metallic toroidal walls surrounding the plasma and pass through the plasma many times at different angles. A complete calculation, there-

Manuscript received May 6, 1974. This work was supported in part by the U.S. Atomic Energy Commission.

R. A. Blanken and D. S. Komm are with the Research Laboratory of Electronics, Massachusetts Institute of Technology, Cambridge, Mass. 02139.

P. Brossier is with the Association Euratom-CEA, Fontenay aux Roses, France.

fore, is extremely difficult to make although the complete calculation is necessary to rigorously ascertain the radiation received by a waveguide antenna. We have therefore chosen to take a simpler approach.

We assume that the Doppler broadening is negligible compared with the field broadening, so that the emission is local; i.e., $\omega = n\omega_c(x)$. There are two limits to consider.

1) Reabsorption is negligible ($\int_{\text{ray path}} \alpha_\omega \, dl \ll 1$), which leads to a single-particle spectrum.

2) Reabsorption dominates ($\int_{\text{ray path}} \alpha_\omega \, dl \gg 1$), which leads to a blackbody spectrum.

Since the emission cannot exceed blackbody, the single-particle emission occurs only if it is smaller than the blackbody level.

For a blackbody spectrum, the radiation received by an antenna of cross-sectional area s is given by

$$dP/d\omega = 2\pi s B_0(\omega) = s[n\omega_c(x)]^2 kT(x)/(4\pi^2 c^2) \quad \text{W(rad/s)}^{-1} \quad (6)$$

where we have assumed that the guide is heavily overmoded so that the free-space result is obtained and the solid angle of reception is 2π sr. The spectrum differs from the usual blackbody result because the local assumption $\omega = n\omega_c(x)$ leads to a variation of the radiation temperature with frequency. Note that the properties of the cavity do not enter this result.

In the opposite limit of a single-particle spectrum the cavity plays an important role. For a large experimental toroidal cavity, the cavity losses are primarily through the holes (of area S) in the wall which are necessary for pumping and diagnostic purposes; losses due to skin effects are negligible. Since the waveguide antenna simply looks like another hole in this limit, the power going down the guide will simply be ($s \ll S$)

$$\frac{dP}{d\omega} = \frac{s}{S}\frac{dP}{d\omega_{\text{plasma}}} = \frac{s}{S}\frac{R_0}{\omega_{co}} 2\pi R \int_{-y}^{+y} j_\omega \, dy \ \text{W(rad/s)}^{-1} \quad (7)$$

where the integral over y is along a line of constant B; the coordinates for the integration are illustrated in Fig. 1.

A plot of the power going down the guide for a receiver with a spatial resolving power of 1 cm, using (6) and (7) and typical Tokamak parameters, is given in Fig. 2 for $s = 1$ cm^2 and $s/S = 10^{-2}$. It is apparent that the first and second harmonics are "black" except near the edges of the plasma where the model breaks down. The third harmonic is "gray:" the two emission levels are similar and which one dominates depends to a large extent on the plasma parameters. The power received by the antenna in the bandwidth of interest amounts to several hundreds of microwatts and should be easily detectible.

Another important feature of the Tokamak spectrum is the overlapping of adjacent harmonics. The criterion for overlapping between harmonic n and harmonic $n + 1$ depends only on the aspect ratio $A = R_0/a$ (see Fig. 1) and is easily shown to be

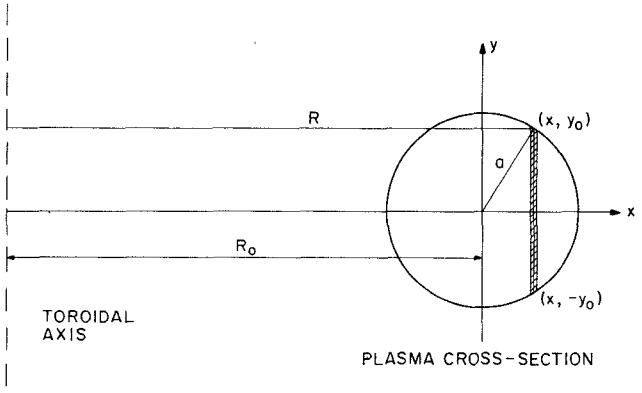

Fig. 1. Tokamak geometry.

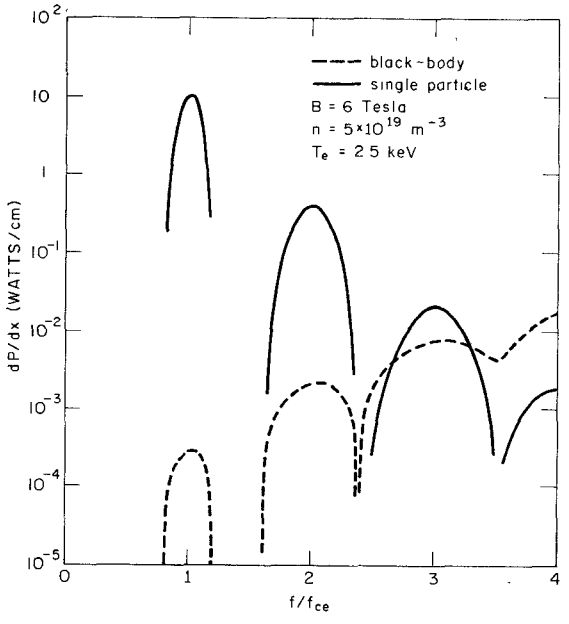

Fig. 2. Synchrotron radiation spectra.

$$n/(n+1) > (A-1)/(A+1). \quad (8)$$

In the regions of overlapping, the power received will be the sum of the individual contributions, so long as the blackbody level is not exceeded.

Several types of diagnostic information are obtainable from the spectrum. In the blackbody region, which usually occurs for the first and second harmonics, the electron temperature profile may be inferred from the data, since the spatial magnetic-field dependence is known. In the single-particle region the intensity varies as $n_e T^n$ which again mainly provides information about the temperature profile. If the electron-distribution function is not Maxwellian, absolute measurement in the blackbody region will show greater than thermal emission, and there may be considerable emission in the frequency gaps in the thermal spectrum (Fig. 2). The measurement of the spectrum may therefore yield information about the suprathermal and runaway electron populations. An instrument capable

of analyzing the experimental spectrum is described in Section III.

III. DESCRIPTION OF THE FAST-SCANNING FABRY–PÉROT INTERFEROMETER

In order to be able to resolve a spectrum on a millisecond time scale with a Fabry–Pérot, it is necessary that one of the reflecting elements be translated through a wavelength in a few milliseconds. We therefore constructed a dynamic Fabry–Pérot by mounting one of the mirrors on a loudspeaker dome (Fig. 3). The construction details and the performance of this instrument have been described elsewhere [7]. In this section we will discuss the properties of this instrument which are pertinent to synchrotron-radiation measurements.

The transmission through a Fabry–Pérot interferometer, with identical mirrors, each having an intensity transmission coefficient t and an intensity reflection coefficient r is given by [8]

$$\tau(\psi) = \tau_{\max}[1 + (2F/\pi)^2 \sin^2 \psi]^{-1} \tag{9}$$

where

$$\tau_{\max} = (1 + a/t)^{-2}, \qquad a = 1 - r - t$$

$$\psi = \phi + Nkd \cos\theta, \qquad F = \pi r^{1/2}(1 - r)^{-1}$$

and where ϕ is the phase change on internal reflection, N the index of refraction of the separating medium, $k = 2\pi/\lambda$, d is the separation of the mirrors, and θ the incidence angle.

The resolving power ρ of the interferometer is given by $\rho = mF$ where m is the order of the interference; the free spectral range $(\Delta\lambda_0)_{sR}$ is given by $(\Delta\lambda_0)_{sR} \doteq \lambda_0/m$. For our application, the desired $(\Delta\lambda_0)_{sR}$ determines the maximum usable order of interference, and so ρ is limited by the highest obtainable value of F.

Two-dimensional metal mesh with square symmetry is the most satisfactory material for fabrication of mirrors for a submillimeter Fabry–Pérot interferometer since it possesses the simultaneous properties of low absorption and high reflectivity for a suitable mesh spacing g. Typically, the ratio λ/g will be $2 < \lambda/g < 10$ for reasonable values of the finesse F and maximum transmission $\tau_{\max}$. For example, using mesh with $\lambda/g = 6.7$, we have obtained a finesse of 42 with a peak transmission of 28 percent. The other physical dimensions of the mesh, the strip width and the mesh thickness, affect the optical properties to a lesser extent than the ratio λ/g.

The dynamic properties of the instrument have been tested, using 337-μm radiation from a hydrogen cyanide laser. A complete order of interference at this wavelength can be scanned in a time as short as 2 ms with no decrease in finesse from the value obtained by scanning the interferometer slowly via the micrometer screw controlling the position of the second mirror. As shorter scan times are used, the finesse decreases slowly. Detailed results are given elsewhere [7].

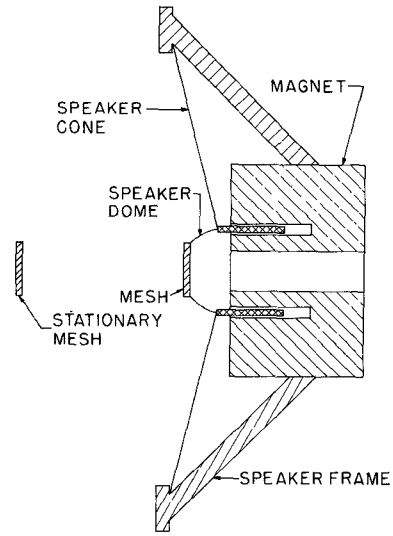

Fig. 3. Fast-scanning Fabry–Pérot interferometer.

Since the spectral range of a given harmonic is $\Delta\lambda = 2\lambda_0/A$, the time required to scan a plasma profile will be approximately 2 ms $\times$ $(2/A)$ $\times$ $(\lambda_0/337)$. For example, for the first harmonic at 6 T, and with an aspect ratio of 5, the time required is 4.3 ms, which is considerably shorter than the experimental Tokamak pulse time.

IV. APPLICATION TO TOKAMAK FAR-INFRARED SPECTROSCOPY

The dominant characteristic of Tokamak synchrotron spectra is the large frequency range resulting from: 1) the simultaneous emission of several harmonics, and 2) the broadening of the individual harmonics due to the inhomogeneous magnetic field (Fig. 2). We have pointed out in Section III that the Fabry–Pérot properties depend upon two experimental parameters λ/d and λ/g. In this section we will show how to choose the proper values of d and g for a given magnetic field B, aspect ratio A, and harmonic number n. In addition, we will discuss the acquisition of experimental data using a fast Fabry–Pérot interferometer and the unfolding of the data to obtain the Tokamak radiation spectrum.

Because of the very large frequency range of the emitted spectrum, we will concentrate on acquisition of data from one individual harmonic at a time. A low enough m must be chosen to insure the following.

1) The free spectral range of the interferometer $(\Delta\lambda_0)_{sR}$ is greater than the width $\Delta\lambda = 2\lambda_0/A$ of a single harmonic, which requires $m < A/2$. This insures that only one order of interference occurs within the spectral width of the scanned harmonic.

2) The contribution from other orders of interference lying in adjacent harmonics do not mask the contribution from the scanned harmonic. The first condition is satisfied

for typical experimental aspect ratios $A \gtrsim 5$ with $m \leq 2$. The second condition is, however, more stringent and indicates that the optimum operation is always obtained by working in the lowest order $m = 1$. For a given magnetic field, the condition $m = 1$ determines that the spacing $d = \lambda/2$.

Working in lowest order would appear to reduce the maximum obtainable resolving power. The spatial resolution $\Delta x = R_0/\rho$, however, is limited by the Doppler and relativistic broadenings. For plasma temperature $T_e \gtrsim$ 1 keV the typical broadening will be several percent. The maximum required resolving power is therefore at most 50, which would be obtained with a finesse of 50 operating in first order. This value of finesse is easily obtained experimentally by choosing an appropriate λ/g (the exact value of λ/g depends upon the strip width and mesh thickness).

It should be pointed out that the operation of the wire-mesh Fabry–Pérot is quite different from that of the standard optical Fabry–Pérot, whose finesse and transmission are almost frequency independent. Because of the mesh properties [9], it can be shown that the finesse varies like λ^2/g^2. Curve 1 in Fig. 4 shows the transmission through a Fabry–Pérot using the result of Saksena *et al.* [9] for the mesh reflectivity and equation (9). The first order of interference has been chosen to analyze the center of the first harmonic. The analysis of the first harmonic requires rejection of all higher orders of interference. The variation of the reflection coefficient r with λ can be used to make a low-pass filter. Curve 2 shows the variation of r at an angle of incidence of 45°, with λ/g adjusted to give minimum reflection in the center of the third harmonic; this choice leads to $r \simeq 90$ percent in the first harmonic. Curve 3 shows the output through a system of four such reflection filters. It is apparent from the figure that the rejection ratio is not large enough for the second harmonic. Therefore, we have added a Fabry–Pérot operating in reflection mode at 45° with its first order of interference in the center of the second harmonic (curve 4). Curve 5 shows the total transmission through the whole system. Since the other components of the system are relatively frequency independent, the relative spectral power is obtained by multiplying curve 5 of Fig. 4 with the spectral power entering the guide shown in Fig. 1; numerical integration of this product shows that the amount of power through the first order peak of the analyzing Fabry–Pérot is at least one order of magnitude greater than all other unwanted spectral contributions. Similar analysis of higher harmonics, $n \geq 2$, will be easier since fewer rejection filters are required.

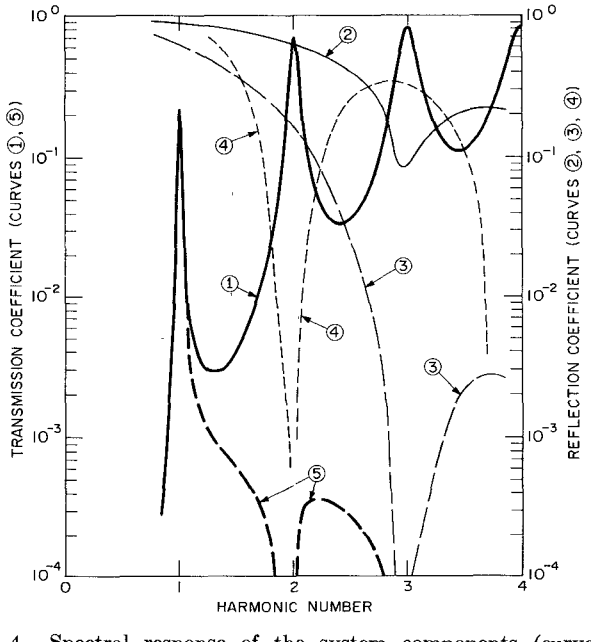

Fig. 4. Spectral response of the system components (curve 1: transmission of the scanning Fabry–Pérot; curve 2: reflection coefficient r from a single mesh at 45°; curve 3: r^4; curve 4: reflection coefficient from a Fabry–Pérot at 45°) and resulting system response (curve 5).

V. CONCLUSION

We have demonstrated the feasibility of measuring the Tokamak synchrotron radiation spectrum using a fast-scanning Fabry–Pérot interferometer. The advantages of this method are as follows.

1) The spatial resolution is limited only by Doppler and relativistic broadenings $\Delta x/R_0 \simeq 0.02$.

2) A complete scan of the plasma can be obtained in less than 5 ms.

3) It requires only one detector.

The difficulties which arise from the variation of the mesh reflectivity with wavelength are: 1) good preselection is required; 2) the convolution of the data is more difficult. This method appears to be the only one using a single detector capable of analyzing the spectrum of a rapidly varying plasma with good spatial resolution.

REFERENCES

[1] G. A. Schott, *Electromagnetic Radiation.* Cambridge, England: Cambridge, 1912.
[2] J. Schwinger, "On the classical radiation of accelerated electrons," *Phys. Rev.*, vol. 75, pp. 1912–1925, June 1949.
[3] G. Bekefi, *Radiation Processes in Plasmas.* New York: Wiley, 1966.
[4] B. A. Trubnikov, "Plasma radiation in a magnetic field," *Sov. Phys.—Dokl.*, vol. 3, pp. 136–140, Jan.–Feb. 1958.
[5] M. N. Rosenbluth, "Synchrotron radiation in Tokamaks," *Nucl. Fusion*, vol. 10, pp. 340–343, Sept. 1970.
[6] F. Engelmann and M. Curatolo, "Cyclotron radiation from a rarefied inhomogeneous magnetoplasma," *Nucl. Fusion*, vol. 13, pp. 497–507, Aug. 1973.
[7] D. S. Komm, R. A. Blanken, and P. Brossier, to be published.
[8] M. A. Born and E. Wolf, *Principles of Optics.* New York: Macmillan, 1964.
[9] B. D. Saksena, D. R. Pahwa, M. M. Pradhan, and K. Lal, "Reflection and transmission characteristics of wire gratings in the far infrared," *Infrared Phys.*, vol. 9, pp. 43–52, July 1969.